

ORIGINAL ARTICLE

Diffusion Tensor Imaging of the Kidneys: Influence of b-Value and Number of Encoding Directions on Image Quality and Diffusion Tensor Parameters

Natalie C. Chuck, Günther Steidle¹, Iris Blume, Michael A. Fischer, Daniel Nanz, Andreas Boss

Department of Diagnostic and Interventional Radiology, University Hospital Zürich, Switzerland, ¹Section of Experimental Radiology, University Hospital of Tübingen, Germany

Address for correspondence:

Dr. Natalie Chuck,
Institute for Diagnostic and Interventional
Radiology, University Hospital Zürich,
Raemistrasse 100, 8091
Zürich, Switzerland.
E-mail: andreas.boss@usz.ch



Received : 06-05-2013

Accepted : 31-08-2013

Published : 28-11-2013

ABSTRACT

Objectives: The purpose of this study was to evaluate to which degree investment of acquisition time in more encoding directions leads to better image quality (IQ) and what influence the number of encoding directions and the choice of b-values have on renal diffusion tensor imaging (DTI) parameters. **Material and Methods:** Eight healthy volunteers ($32.3 \text{ y} \pm 5.1 \text{ y}$) consented to an examination in a 1.5T whole-body MR scanner. Coronal DTI data sets of the kidneys were acquired with systematic variation of b-values (50, 150, 300, 500, and 700 s/mm^2) and number of diffusion-encoding directions (6, 15, and 32) using a respiratory-triggered echo-planar sequence (TR/TE 1500 ms/67 ms, matrix size 128×128). Additionally, two data sets with more than two b-values were acquired (0, 150, and 300 s/mm^2 and all six b-values). Parametrical maps were calculated on a pixel-by-pixel basis. Image quality was determined with a reader score. **Results:** Best IQ was visually assessed for images acquired with 15 and 32 encoding directions, whereas images acquired with six directions had significantly lower IQ ratings. Image quality, fractional anisotropy, and mean diffusivity only varied insignificantly for b-values between 300 and 500 s/mm^2 . In the renal medulla fractional anisotropy (FA) values between 0.43 and 0.46 and mean diffusivity (MD) values between $1.8\text{-}2.1 \times 10^{-3} \text{ mm}^2/\text{s}$ were observed. In the renal cortex, the corresponding ranges were 0.24-0.25 (FA) and $2.2\text{-}2.8 \times 10^{-3} \text{ mm}^2/\text{s}$ (MD). Including b-values below 300 s/mm^2 , notably higher MD values were observed, while FA remained constant. Susceptibility artifacts were more prominent in FA maps than in MD maps. **Conclusion:** In DTI of the kidneys at 1.5T, the best compromise between acquisition time and resulting image quality seems the application of 15 encoding directions with b-values between 300 and 500 s/mm^2 . Including lower b-values allows for assessment of fast diffusing spin components.

Key words: Diffusion tensor imaging, diffusion weighted imaging, kidneys

Access this article online

Quick Response Code:



Website:

www.clinicalimaging-science.org

DOI:

10.4103/2156-7514.122323

Copyright: © 2013 Chuck NC. This is an open-access article distributed under the terms of the Creative Commons Attribution License, which permits unrestricted use, distribution, and reproduction in any medium, provided the original author and source are credited.

This article may be cited as:
Chuck NC, Steidle G, Blume I, Fischer MA, Nanz D, Boss A. Diffusion Tensor Imaging of the Kidneys: Influence of b-Value and Number of Encoding Directions on Image Quality and Diffusion Tensor Parameters. J Clin Imaging Sci 2013;3:53.
Available FREE in open access from: <http://www.clinicalimaging-science.org/text.asp?2013/3/1/53/122323>

INTRODUCTION

There is an increasing number of methods for functional imaging of the kidneys,^[1] e.g. dynamic MRI with gadolinium-based contrast media, diffusion weighted imaging (DWI),^[2-5] blood-oxygenation level dependent imaging (BOLD),^[6,7] arterial spin labeling (ASL),^[8,9] and MR-elastography.^[10-12]

DWI can help in the detection of renal abnormalities^[3,13-15] and characterization of focal renal lesions^[16] using the apparent diffusion coefficient (ADC). The ADC can be quantitatively measured and holds information on the degree of free or restricted Brownian water diffusion.^[17]

In diffusion tensor imaging (DTI), the diffusion-induced signal attenuation is measured for water displacement along at least six non-collinear directions. This allows a full description of the second-rank diffusion tensor and a quantitative assessment of diffusion anisotropy. Biological structures, such as the tubuli in the kidneys may restrict the Brownian motion of the water molecules in a direction dependent manner and cause anisotropy of the diffusion.^[18] Renal structures in the medulla are oriented in a radial fashion resulting in stronger anisotropy effects in the medulla than in the cortex.^[19]

It was previously shown that a larger number of encoding directions may result in improved accuracy of diffusion tensor analysis in the brain.^[20,21] For DTI of the kidneys it is still unclear what number of encoding directions and what range of b-values should be chosen during acquisition time to optimize image quality. The aim of this study was to evaluate whether investment of acquisition time in a higher number of encoding directions results in improved image quality and more robust DTI parameters, to identify the optimal b-value for DTI of the kidneys, and to investigate how DTI parameters change if more than two b-values are applied.

MATERIALS AND METHODS

Subjects

After approval by the ethics committee, 8 healthy volunteers (4 females, age between 24 and 41 y, mean age $32.3 \text{ y} \pm 5.1 \text{ y}$) without any history of kidney disease, diabetes, hypertension or vascular disease, agreed to the examination. No specific preparations such as fasting or drinking were undertaken prior to the examination.

Imaging Protocol

All examinations were performed on a 1.5 T whole body scanner (Philips Achieva, Philips Healthcare, Best, The Netherlands) using a phased-array coil with 32 elements,

consisting of a 16 element anterior and a 16 element posterior coil.

After a gradient-echo localizer, morphological imaging sequences were acquired in a 22-second breath-hold using balanced gradient-echo sequences (TR 3.45 ms/TE 1.73 ms/flip angle 90°) in all three directions to provide anatomical orientation for diffusion imaging and to check for morphological abnormalities.

Diffusion tensor images were acquired in oblique-coronal orientation with a respiratory-triggered (respiratory belt) fat-saturated single spin-echo echo-planar imaging sequence (TR 1500 ms/TE 67 ms, flip angle 90° , bandwidth 2168 Hz/px) along the longest axis of the kidneys.

The angle of the oblique-coronal plane was adjusted manually for both kidneys in each subject, to identify the longest axis [Figure 1a]. In cases where the angles of the kidneys differed from each other, a compromise between the longest axes of both was used.

The DTI acquisitions were repeated with 6, 15 and 32 diffusion encoding directions and a fixed b-value of 500 s/mm^2 . Additional data sets were then acquired with b-values of 50, 150, 300, and 700 s/mm^2 and a fixed number of encoding directions of 15 (overview of the different schemes in Table 1). The number of encoding directions (6, 15 and 32) was the standard selection to choose from provided by the manufacturer.

The remaining parameters were as follows: 3 slices; slice thickness 4 mm with no intersection gap; TR/TE 1500 ms/67 ms; bandwidth in EPI frequency direction 2168 Hz/pixel; field of view $384 \times 384 \text{ mm}^2$; matrix size 128×128 ; in-plane voxel size $3 \times 3 \text{ mm}^2$; partial Fourier factor 6/8, averages 3; phase encoding direction left to right. The acquisition was accelerated by parallel imaging (SENSE) with a factor of 4. SENSE factor had to be chosen relatively high to reduce susceptibility artifacts. Bandwidth was set

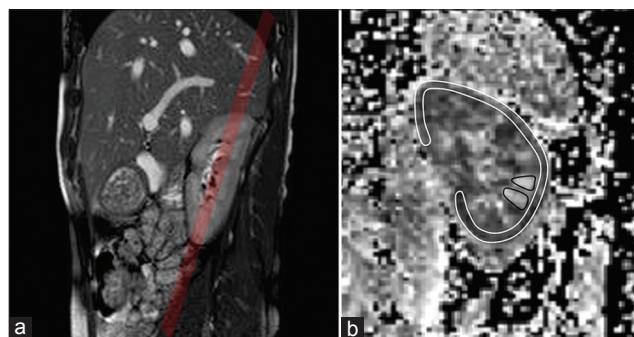


Figure 1: (a) Exemplary image to illustrate the orientation of the oblique-coronal plane. (b) Typical ROI placement in a fractional anisotropy map ($b = 300 \text{ s/mm}^2$, 15 encoding directions).

Table 1: Overview of the different evaluation schemes

Sequence	Field strength	TR (ms)	TE (ms)	Bandwidth (Hz/px)	Voxel size (mm)	Number of averages	Slices	b-values (s/mm ²)	Number of encoding directions
2b 6d b500	1.5 T	1500	67	2168	3 x 3 x 3	3	3	0, 500	6
2b 15d b300								0, 300	15
2b 15d b500								0, 500	15
2b 15d b700								0, 700	15
2b 32d b500								0, 500	32
3b 15d								0, 50, 300	15
6b 15d								0,50,150,300,500,700	15

All parameters, except for the b-values and the number of encoding directions were left unchanged

at maximum to reduce image distortions due to magnetic field inhomogeneities as far as possible. Fat saturation using SPIR was used to minimize chemical-shift artifacts.

Due to the use of a respiratory belt, acquisition time was dependent on the respiratory rate of each individual. Acquisition time for the whole protocol was between 60 and 80 min [Table 2]. It was not the aim of this study to compare a different number of encoding directions using the same acquisition time, as it is known that the acquisition of more encoding directions is advantageous over averaging.

Post processing

The averaged diffusion-weighted images were analyzed using adapted routines written in Matlab (The Mathworks, Inc., Natick, MA, USA). The diffusion tensor elements were evaluated as reported by Basser^[22] on a pixel-by-pixel basis. A mono-exponential signal decay curve was fitted to the signal intensities. A conventional fit was performed using 2 b-values for the data sets with b = 300, 500, and 700 s/mm² and 15 encoding directions as well as for 6 and 32 encoding directions with b = 500 s/mm². Additionally, two evaluation schemes with data acquired with more than two b-values and 15 encoding directions were applied: In one evaluation scheme data acquired with 3 b-values (0, 50, 300 s/mm²) and in another scheme with all 6 b-values (0, 50, 150, 300, 500, and 700 s/mm²) were included in the fitting analysis. After calculation of the diffusion tensor, the tensor was diagonalized and parametrical maps were calculated starting from the computed principal diffusivity components, D₁, D₂, and D₃. The fractional anisotropy is defined as

$$FA = \frac{\sqrt{3(D_1 - MD)^2 + (D_2 - MD)^2 + (D_3 - MD)^2}}{\sqrt{(2D_1^2 + D_2^2 + D_3^2)}}$$

with the mean diffusivity being defined as

$$MD = \frac{D_1 + D_2 + D_3}{3} \quad [22]$$

Table 2: Acquisition time

Sequence	b-value	Acquisition time
GRE localizer		3 min 20 s
BTFE-BH axial		1 min 07 s
BTFE-BH sagittal		2 min 14 s
BTFE-BH coronal		3 min 00 s
DTI 2b 6d	500	
DTI_RT 2b 15d	50, 150, 300, 500, 700	approx. 4-7 min per b-value
DTI 2b 32d	500	
Overall acquisition time		~60-80 min

Total acquisition time for each individual ing rate during the acquisition of the respiratory-triggered DTI sequences using a respiratory belt. DTI: Diffusion tensor imaging, GRE: Gradient Echo, BTFE-BH: Balanced Turbo Field Echo in Breath Hold

The fractional anisotropy is a quantitative measure for the “mean orientedness” of the diffusion-hindering microstructures in a voxel. If those structures allow diffusion only along a single direction, a maximum FA value of 1 is expected, whereas completely free or isotropically restricted diffusion should result in a FA of 0. The MD is a measure for the overall presence of obstacles to diffusion. The MD is a superior quantitative measure compared to averaging the ADC in three orthogonal directions as the diffusion anisotropy is completely accounted for. A high MD can be computed in water-like fluid, in which free diffusion occurs.^[23]

For quantitative evaluation of FA and MD one continuous region-of-interest (ROI) was drawn over the cortex, aiming to cover the whole cortex and two separate ROIs were placed in two different medullar areas, chosen as large as possible, on the parametrical maps [Figure 1b]. All ROI definitions were performed on parametrical maps of mean diffusivity and subsequently copied to the DTI maps. Slices including large renal vessels were not selected to avoid flow related artifacts. The mean and the standard deviation of the obtained FA and MD values were computed. The same ROIs were used to measure both, FA and MD measurements.

Assessment of image quality

Both kidneys were used for image analysis. Image quality of the FA and MD maps was assessed by two authors (I.B. and M.A.F.) in consensus. Visual assessment was performed in

consensus reading using an ordinal 4-point scale. The overall image quality for MD and FA maps was assessed taking into account: Corticomedullar discrimination, distortion, motion, and susceptibility artifacts. For graduation, a 4-point-scale was applied:^[24]

- 1 = Poor corticomedullar differentiation
- 2 = Moderate corticomedullar differentiation
- 3 = Good corticomedullar differentiation
- 4 = Excellent corticomedullar differentiation

SNR measurements

To measure the minimum signal-to-noise-ratio (SNR) of the kidney medulla and cortex, a ROI was placed in the medulla of the left kidney using the $b = 0$ s/mm² image and copied to all DTI images (15 directions) of that slice for the b-values of 300, 500, and 700 s/mm². The SNR was defined as the lowest signal intensity of the renal medulla or cortex in the 15 diffusion directions divided by the standard deviation of the background noise. Background noise was relatively stable for the different b-value measurements (300, 500, and 700 s/mm²). Therefore, we defined a relative SNR and CNR as SNR* and CNR* within each subject, which seems valid even in case of parallel image acquisition and corresponded well to the visual impression. CNR* was calculated using the following formula:

$$CNR = |SNR^*_{(Cortex)} - SNR^*_{(Medulla)}|$$

Statistical analysis

After testing for normal distribution, Student's *t*-test was used to compare the individual cortical and medullar FA and MD of healthy volunteers. The different evaluation schemes were statistically tested in comparison to the standard evaluation scheme with 15 different encoding directions using two b-values with the lower b-value = 0 and the higher b-value = 500 s/mm². All statistical tests were performed on log-transformed values to increase normal distribution. Analysis was performed with SPSS 19.0 (SPSS, Inc., Chicago, IL) and Excel 2003/2008 (Microsoft, Redmond, WA).

RESULTS

Each volunteer was scanned successfully and except for a sporadic cyst in one of the male volunteers, no morphologic abnormalities were found.

Assessment of image quality

FA maps acquired with more than 6 encoding directions (2b 15d b500, 2b 32d b500) showed significantly better image quality ($P < 0.05$) compared to only six encoding directions (2b 6d b500). No significant differences were found for MD maps for different encoding directions (2b 6d b500, 2b 15d b500 and 2b 32d b500) [Figures 2 and 3].

Parametrical maps of MD exhibited good image quality ranked between 2.5 and 3.3 on the 4-point scale [Table 3]. MD maps were relatively robust regarding susceptibility artifacts compared to the FA maps, which often exhibited susceptibility related artifacts in the upper pole of the left kidney [Figure 4]. Due to the susceptibility related artifacts, quality of FA maps (1.5-2.6 on the 4-point scale) were ranked inferior ($P < 0.05$) compared to the corresponding MD maps (2.5-3.3 on the 4-point-scale).

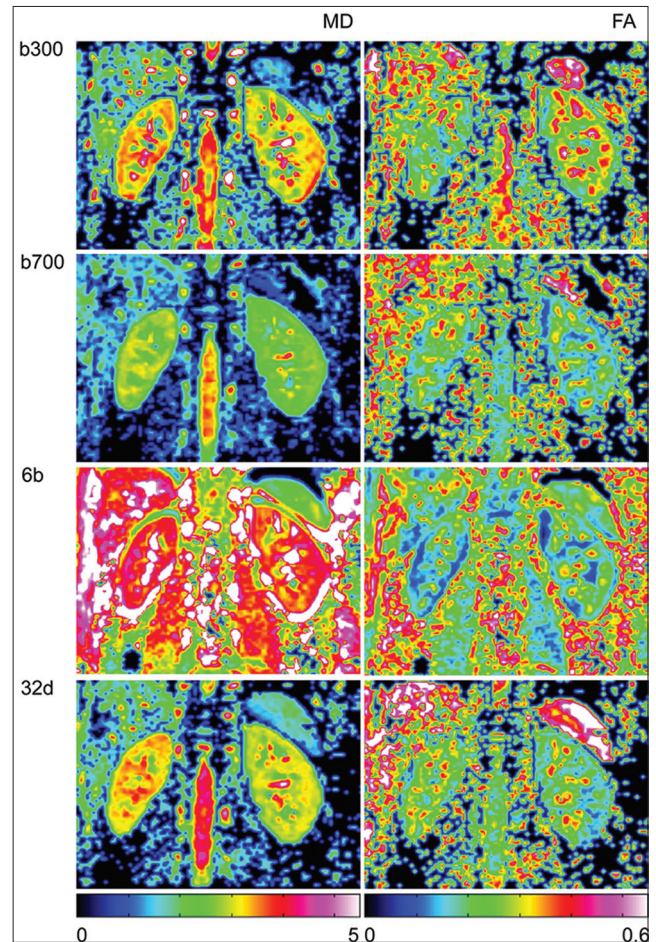


Figure 2: Comparison of image quality of FA and MD maps: Upper two rows were calculated with two b-values: $b = 0$ and b-values of 300 and 700 s/mm² using 15 encoding directions (2b 15d b300 and 2b 15d b700). Third row with all 6 b-values with 15 encoding directions. In the parametrical MD map computed from 6 b-values, markedly increased diffusion is displayed without significant alterations in the FA maps compared to the parametrical images of the upper row.

Table 3: Assessment of image quality		
	FA-Maps	MD-Maps
2b 6d b500	1.5 ± 0.5	2.5 ± 0.9
2b 15d b300	2.63 ± 0.7	3.0 ± 0.5
2b 15d b500	2.38 ± 0.5	3.13 ± 0.6
2b 15d b700	2.13 ± 0.4	3.25 ± 0.9
2b 32d b500	2.13 ± 0.3	2.75 ± 0.7

Image quality of parametrical MD and FA maps for the different evaluation schemes. Visual assessment was performed by two readers in consensus using an ordinal 4-point-scale. FA: Fractional anisotropy, MD: Mean diffusivity

Quantitative evaluation of FA and MD values of the kidney cortex and medulla

The computed mean values and standard deviations for the different evaluation schemes are displayed in Table 4.

Influence of number of encoding directions on MD

Using the evaluation scheme applying only 6 encoding directions (2b 6d b500), MD values in the medulla ($1.87 \pm 0.12 \times 10^{-3} \text{ mm}^2/\text{s}$) were significantly

lower ($P < 0.05$) compared to the evaluation scheme with 15 encoding directions (2b 15d b500). No statistically significant difference was found regarding medullary MD comparing 15 and 32 encoding directions. Furthermore, no difference was found for cortical MD for all numbers of encoding directions.

Influence of b-value scheme on MD

MD was significantly higher ($P < 0.05$) in the cortex than in the medulla when evaluation schemes (2b 6d b500, 2b 15d b500, 2b 32d b500) applying two b-values were used. In contrast, MD of the cortex was significantly lower ($P < 0.05$) than in the medulla for the two evaluation schemes applying more than 2 b-values (3b 15d, 6b 15d). Compared to the schemes with 2 b-values and lower second b-value (2b 15d b300 and 2b 15d b500), choosing a higher b-value of 700 s/mm² (2b 15d b700) resulted in lower MD of the medulla and the cortex ($P < 0.01$).

Influence of b-value scheme and number of encoding directions on FA

The fractional anisotropy (FA) of the medulla was significantly higher than in the cortex ($P < 0.05$) in all evaluation schemes. FA values in the cortex showed no significant difference ($P > 0.05$) between evaluation schemes (2b 15d b300, 2b 15d b500, 2b 15d b700) as well as in the evaluation scheme using more than two b-values (3b 15d, 6b 15d) and 6 and 32 encoding directions (2b 6d b500 and 2b 32d b500).

Signal-to-noise and contrast-to-noise ratio

Signal-to-noise (SNR) was higher in the cortex than in the medulla and highest in the scheme with $b = 300 \text{ s/mm}^2$ at 15 directions (2b 15d b300). All evaluation schemes taken into consideration for SNR measurements, except for the SNR of the medulla with $b = 700 \text{ s/mm}^2$ (2b 15d b700), showed SNR values above 10 as shown in [Figure 5]. Contrast-to-noise (CNR) ratio was almost the same for

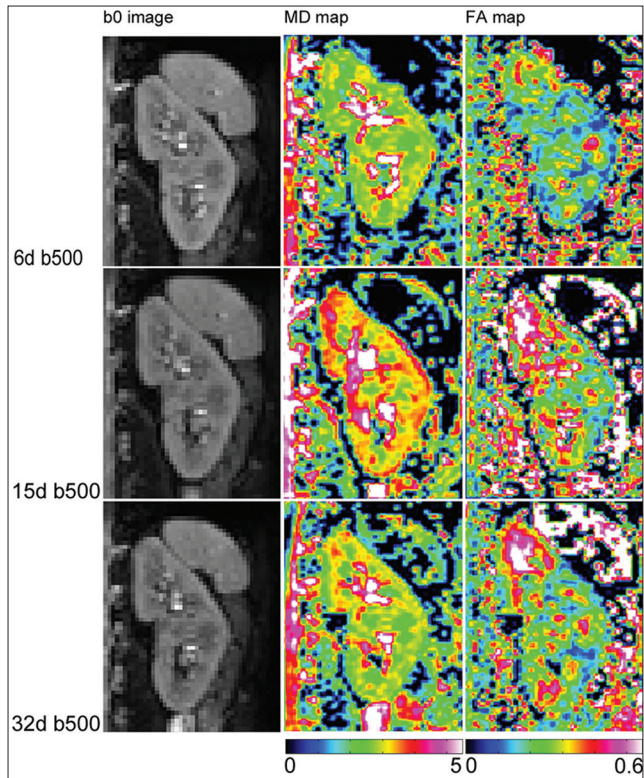


Figure 3: Comparison of image quality of FA and MD maps with the different encoding directions: The upper row shows the b0 image, the MD and FA map with 6 encoding directions with b-value 0 and 500 s/mm², the second row shows the same order with 15 encoding directions with b-value 0 and 500 s/mm² and the third row shows the b0 image, MD and FA map with 32 encoding directions, again with b-values 0 and 5 s/mm². Best corticomedullary discrimination is seen with 15 directions.

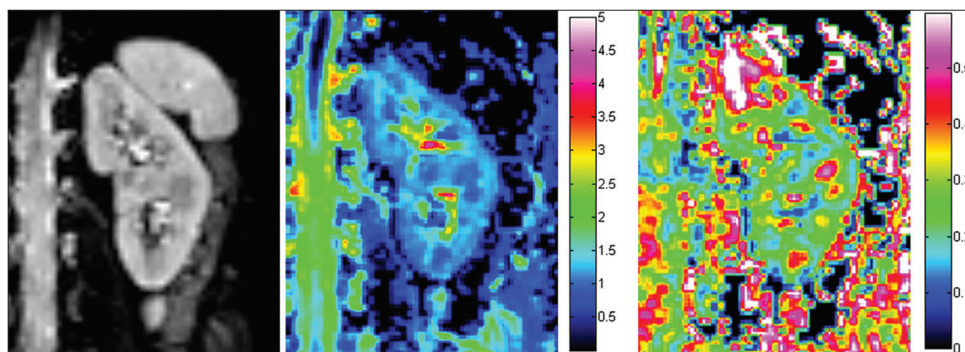


Figure 4: Left side: $b = 0 \text{ s/mm}^2$ image of the left kidney. Corresponding parametrical MD map (center) and FA map (right side) acquired with a b-value of 500 and 15 encoding directions (2b 15d b500). $B = 0 \text{ s/mm}^2$ image and MD map show no significant artifacts, whereas in the FA map severe artifacts are visible in the upper pole of the kidney.

Table 4: Quantitative assessment of FA and MD

	FA Medulla	FA Cortex	MD Medulla [$10^{-3} \text{ mm}^2/\text{s}$]	MD Cortex [$10^{-3} \text{ mm}^2/\text{s}$]
2b 6d (b=0, 500 s/mm ²)	0.46 ± 0.02	0.25 ± 0.01	1.87 ± 0.12*	2.50 ± 0.12
2b 15d (b=0, 300 s/mm ²)	0.43 ± 0.02	0.25 ± 0.02	2.14 ± 0.33	2.78 ± 0.37
2b 15d (b=0, 500 s/mm ²)	0.45 ± 0.01	0.25 ± 0.01	2.05 ± 0.26	2.63 ± 0.33
2b 15d (b=0, 700 s/mm ²)	0.44 ± 0.01	0.25 ± 0.01	1.82 ± 0.21*	2.23 ± 0.18*
2b 32d (b=0, 500 s/mm ²)	0.45 ± 0.02	0.25 ± 0.01	1.97 ± 0.25	2.79 ± 0.28
3b 15d (b 0, 50, 300 s/mm ²)	0.44 ± 0.02	0.24 ± 0.01	3.58 ± 0.15*	2.73 ± 0.27
6b 15d (b=0, 50, 150, 300, 500, 700 s/mm ²)	0.43 ± 0.01	0.25 ± 0.01	3.23 ± 0.40*	2.41 ± 0.33

Mean FA and MD of renal medulla and cortex. Evaluation schemes were compared to the scheme with 15 encoding directions and b-value of 500 s/mm². Significant differences ($P < 0.05$) are indicated with "*". FA: Fractional anisotropy, MD: Mean diffusivity

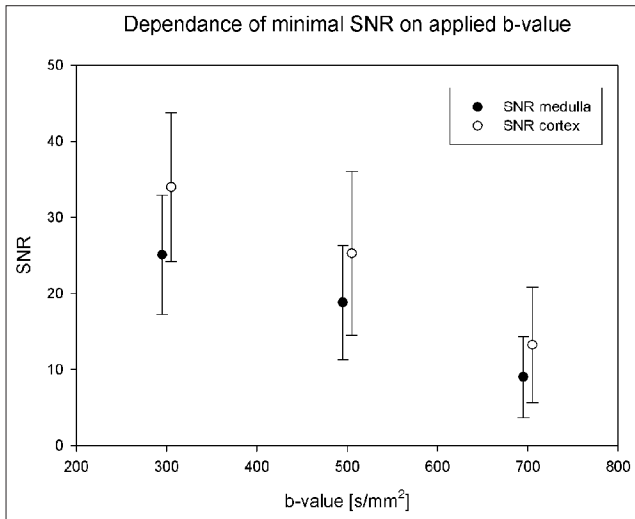


Figure 5: Minimal signal-to-noise ratio (SNR) decreases with increasing b-value. A b-value of 700 s/mm² results in low SNR with an underestimation of mean diffusivity and degradation of image quality.

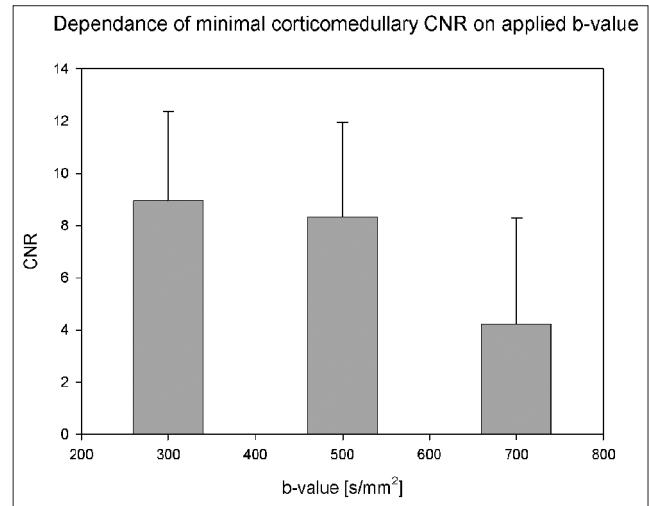


Figure 6: Corticomedullary contrast-to-noise-ratio (CNR) remains stable for b-values between 300 and 500 s/mm², whereas a b-value of 700 s/mm² leads to a reduction of CNR.

evaluation schemes with 15 directions and b-values b = 0, 300 s/mm² and b = 0, 500 s/mm² (2b 15d b300 and 2b 15d b500) were significantly higher ($P < 0.05$) than in the evaluation scheme with 2 b-values, 15 encoding directions and b-values = 0, 700 s/mm² (2b 15d b700) [Figure 6].

DISCUSSION

Our results show that for DTI of the kidney at 1.5T, the best compromise between acquisition time and image quality seems to be the application of b-values between 300 and 500 s/mm² combined with 15 encoding directions. Quantitative evaluation using two b-values (0 and 300 or 500 s/mm²) showed comparable mean values for MD and FA as previously published.^[5,19,24,25]

Image quality and number of encoding directions

Besides the evaluation scheme with six directions (2b 6d b500), all evaluation schemes showed good image quality. Except for the number of encoding directions, all imaging parameters have been kept constant, therefore, this scheme had the smallest number of image acquisitions with the shortest acquisition time (only about 60% of the acquisition time of the scheme

with 15 diffusion directions); therefore signal-to-noise is about 50% less comparing to the scheme with 15 encoding directions. It is conceivable that using more averages could lead to better image quality even with 6 directions, which was, however, not the aim of this study.

In accordance to previous studies better image quality was achieved using more than 6 directions with slightly improved image quality at 15 encoding directions compared to 32 encoding directions.^[19] This might be due to the duration of the scheme as regular breathing is mandatory to achieve good image quality and irregularities in breathing lead to increased motion artifacts and misregistration. We noticed a better image quality in both the FA and the MD maps unlike reported by Notohamiprodo et al., who described significantly better image quality at 12 encoding directions only for the FA maps with significantly lower cortical FA values and slightly lower medullar FA values.^[24]

MD maps exhibited notably better image quality as compared to the FA maps, which may be caused by the higher complexity of diffusion information of the FA maps and subsequent higher susceptibility to imaging artifacts,

whereas the MD maps showed a high robustness. Especially at the upper pole of the left kidney, inhomogeneities of the static magnetic field frequently resulted in a loss of information of diffusion directionality in the FA maps without significant artifacts in MD maps.

Apart from artifacts caused by magnetic field inhomogeneities, slight motion-related artifacts were visible in some of the parametrical maps. Due to the numerous evaluation schemes of this study, overall measurement time (including morphological sequences) was relatively long for each volunteer (between 60 and 80 min, depending on individual respiratory rate). We decided to apply a respiratory triggering technique allowing the acquisition of multiple images during one breathing cycle. As image quality seemed sufficient, we abstained from further techniques for motion compensation such as co-registering of the data sets during post-processing. Further improvement of image quality may be achieved with the application of a navigator triggering technique, which could be applied as an alternative with the echo-planar diffusion sequence instead of a breathing belt, however, resulting in longer measurement time as only one image is acquired per respiration cycle.

Choice of b-value

Best image quality was achieved using two b-values with the higher b-value either 300 or 500 s/mm². Previous studies have claimed that optimal b-values for the kidney lie between 300 s/mm²,^[19,24,26,27] 390 s/mm²,^[28] and 400 s/mm².^[25] Our study confirmed these findings. The b-value of 700 s/mm² resulted in a notable underestimation of MD as compared to the other evaluation schemes. This finding may be explained with the low SNR (<10) in the diffusion weighted images from the different encoding directions using a b-value of 700 s/mm². Interestingly, FA of the renal cortex and medulla remained unchanged, showing that all diffusion directions are similarly affected by the low SNR.

The measured MD is influenced by the choice of b-values, as diffusion weighted imaging exhibits monoexponential signal decay only over a certain range of b-values. The ADC (MD) of the kidney is much higher than those of other organs and has been commonly reported to be between 2.5 and 2.9 mm²/s.^[29] Including lower b-values (3b 15d, 6b 15d) in the diffusion evaluation (0, 50, 300 s/mm² and 0, 50, 150, 300, 500 and 700 s/mm²) measured MD values were significantly higher compared to the other evaluation schemes as well as compared to literature results. It was previously described that low b-values may result in overestimation of mean diffusivity (or ADC) due to

perfusion effects.^[30,31] This is explained by the fact that when applying higher b-values, the faster spin ensembles are already dephased and cannot contribute to the signal; using lower b-values, the contribution of faster moving spins to the MD is included in the measurement, resulting in higher values in the medulla than in the cortex due to faster spins. However, we found similar morphology in the MD maps compared with the evaluation schemes including only higher b-values without strong emphasis of the vascular pattern. Furthermore, the corresponding FA maps exhibited similar anisotropy values in the renal cortex and medulla as in the schemes with only higher b-values. These findings suggest that inclusion of small b-values in the DTI evaluation scheme potentially may allow differentiating slow and fast diffusing spins in the renal medulla, in which the slow diffusing spins might be located in the renal tubuli and the faster diffusing spins in the renal collecting ducts.

Our findings are in line with previous reports on contributions of fast and slow components to the DWI signal. A bi-exponential model has been proposed to more accurately distinguish between these components in the analysis; the most sophisticated approach seems the methodology of intravoxel incoherent motion (IVIM).^[30,32-34] In this study, we were not able to apply the complete IVIM methodology for DTI: For a stable separation of both, perfusion and diffusion effects, a higher number of low b-values between 0 and 100 s/mm² would have been necessary for each of the different spatial encoding directions, which was out of the scope of this study due to limited measurement time.

LIMITATIONS

Our study shows several limitations. First we included a limited number of subjects in this methodological study of image optimization. It is possible that using a higher number of subjects, statistically significant differences between 15 and 32 encoding directions could have been found. None of the subjects' urine or blood was analyzed prior to image acquisition. None of the subjects had a history of renal disease and except for one uncomplicated renal cyst, no morphological abnormalities were found on our images.

Second, to reduce overall measurement time, we used a respiratory belt. Kidney movement is not necessarily in optimal agreement with movements of the abdominal wall as they mainly move in a cranio-caudal direction. The result can be misregistration of respiratory motion that could probably be further reduced by using a navigator triggering technique though resulting in longer acquisition time.

Third, we did not consider motion artifacts caused by arterial pulsatility in this study that would have led to a further increase of acquisition time. There were several studies that have taken this into account^[28] whereas others pursued their studies without pulsatile-triggering due to prolonged acquisition time when combined with respiratory triggering.^[24,26]

Fourth, we did not take hydration status into account, but it can be assumed, as no specific preparations such as fasting or drinking were undertaken, that the hydration state of the kidneys was similar. Muller et al., stated that the hydration state has a significant influence on ADC values;^[35] this was not confirmed in later studies by Damasio et al., and Carbone et al., who did not find any significant changes in ADC values in their study.^[3,36] A couple of years later, Sigmund et al., published a study where they assessed the reproducibility and the distribution of IVIM and DTI parameters before and after hydration and furosemide challenges and they were able to show that the diffusion MR metrics are sensitive to flow changes in the kidney; their results suggest that vascular flow, tubular dilation, water reabsorption, and the intratubular flow all play an important role in DWI contrast.^[37]

Toeny et al., showed that especially acute ureteral obstruction leads to a decrease in ADC values and that these findings might correlate with the decrease in glomerular filtration rate (GFR).^[36] As we just observed healthy volunteers, this as well as the potential effect of urine flow in general was not an issue in our study but may become important in the evaluation of patients with urological pathologies.

Fifth, we used parallel imaging. It is known that quantitative SNR measurement is compromised by the use of parallel imaging. Based on the visual aspect and the intraindividual measured SNR values being relatively constant, we defined a relative SNR* and CNR*.

Sixth, a relatively high parallel imaging factor (SENSE factor 4) was applied to keep susceptibility artifacts (image distortions, signal dephasing) as low as possible with the applied single spin-echo diffusion EPI sequence. Other manufacturers apply double spin-echo diffusion EPI sequences. By adding additional RF refocusing pulses to the SE diffusion sequence and hereby splitting the field gradient pulses into shorter pulses of alternating polarity, a reduction of eddy current artifacts can be achieved.^[38]

Seventh, a coronal slightly oblique slice for depiction of both kidneys within one acquisition was chosen. In all our subjects, the visualization of both poles of each kidney was possible within one image. However, especially in

young female women with low fat in the renal bed, the orientation of both kidneys could notably differ hampering the depiction in coronal orientation.

Eighth, the applied TR of 1.5 sec of the applied diffusion sequence is quite short and using a longer TR might have resulted in better SNR. For practicability, we kept TR short to keep the overall examination time acceptable. In a clinical study, a longer TR in the order of a few seconds seems advantageous.

Ninth, the parametrical maps have been calculated directly without using a postprocessing algorithm for co-registration.

CONCLUSION

In conclusion, in this study we were able to confirm that optimal b-values for DTI of the kidney range between 300 and 500 s/mm² and that increasing the number of encoding directions lead to better image quality as a result of improved corticomedullar discrimination, taking longer acquisition times into account. MD maps are significantly more robust regarding susceptibility artifacts than FA maps. Higher b-values result in underestimation of MD, most likely due to low SNR. Inclusion of low b-values in the evaluation scheme has the potential for distinguishing slow and fast diffusing water in the renal tubuli and collecting ducts, respectively, resulting in higher MD values compared to conventional diffusion evaluation schemes.

Altogether, the number of encoding schemes influences image quality while keeping DTI indices stable. The increase in image quality allows for a more precise data evaluation when placing ROIs for FA and MD measurements. The use of DTI for evaluation of focal and diffuse kidney diseases will have to be assessed in further studies.

ACKNOWLEDGMENTS

We would like to thank Olivio Donati, MD for his valuable support with the application for ethics approval and Roger Lüchinger, PhD, for his help and assistance with the protocol.

REFERENCES

1. Michaely HJ, Herrmann KA, Nael K, Oesingmann N, Reiser MF, Schoenberg SO. Functional renal imaging: Nonvascular renal disease. *Abdom Imaging* 2007;32:1-16.
2. Lorenz CH, Powers TA, Partain CL. Quantitative imaging of renal blood flow and function. *Invest Radiol* 1992;27 Suppl 2:S109-14.
3. Carbone SF, Gaggioli E, Ricci V, Mazzei F, Mazzei MA, Volterrani L. Diffusion-weighted magnetic resonance imaging in the evaluation of renal function: A preliminary study. *Radiol Med* 2007;112:1201-10.
4. Zhang J, Tehrani YM, Wang L, Ishill NM, Schwartz LH, Hricak H. Renal masses: Characterization with diffusion-weighted MR imaging: A preliminary experience. *Radiology* 2008;247:458-64.

5. Thoeny HC, De Keyzer F, Oyen RH, Peeters RR. Diffusion-weighted MR imaging of kidneys in healthy volunteers and patients with parenchymal diseases: Initial experience. *Radiology* 2005;235:911-7.
6. Gloviczki ML, Glockner J, Gomez SI, Romero JC, Lerman LO, McKusick M, et al. Comparison of 1.5 and 3 T BOLD MR to study oxygenation of kidney cortex and medulla in human renovascular disease. *Invest Radiol* 2009;44:566-71.
7. Thoeny HC, Zumstein D, Simon-Zoula S, Eisenberger U, De Keyzer F, Hofmann L, et al. Functional evaluation of transplanted kidneys with diffusion-weighted and BOLD MR imaging: Initial experience. *Radiology* 2006;241:812-21.
8. Michaely HJ, Schoenberg SO, Itrich C, Dikow R, Bock M, Guenther M. Renal disease: Value of functional magnetic resonance imaging with flow and perfusion measurements. *Invest Radiol* 2004;39:698-705.
9. Martirosian P, Boss A, Schraml C, Schwenzler NF, Graf H, Claussen CD, et al. Magnetic resonance perfusion imaging without contrast media. *Eur J Nucl Med Mol Imaging* 2010;37 Suppl 1:S52-64.
10. Mannelli L, Valentino M, Laffi G, Lomas DJ, Sigmund EE, Raz E, et al. [Functional MRI of the kidney]. *G Ital Nefrol* 2010;27:599-608.
11. Mannelli L, Maki JH, Osman SF, Chandarana H, Lomas DJ, Shuman WP, et al. Noncontrast functional MRI of the kidneys. *Curr Urol Rep* 2012;13:99-107.
12. Korsmo MJ, Ebrahimi B, Eirin A, Woollard JR, Krier JD, Crane JA, et al. Magnetic resonance elastography noninvasively detects in vivo renal medullary fibrosis secondary to swine renal artery stenosis. *Invest Radiol* 2013;48:61-8.
13. Palmucci S, Mauro LA, Veroux P, Failla G, Milone P, Ettorre GC, et al. Magnetic resonance with diffusion-weighted imaging in the evaluation of transplanted kidneys: Preliminary findings. *Transplant Proc* 2011;43:960-6.
14. Paudyal B, Paudyal P, Tsuchima Y, Oriuchi N, Amanuma M, Miyazaki M, et al. The role of the ADC value in the characterisation of renal carcinoma by diffusion-weighted MRI. *Br J Radiol* 2010;83:336-43.
15. Chan JH, Tsui EY, Luk SH, Fung SL, Cheung YK, Chan MS, et al. MR diffusion-weighted imaging of kidney: Differentiation between hydronephrosis and pyonephrosis. *Clin Imaging* 2001;25:110-3.
16. Kim S, Jain M, Harris AB, Lee VS, Babb JS, Sigmund EE, et al. T1 hyperintense renal lesions: Characterization with diffusion-weighted MR imaging versus contrast-enhanced MR imaging. *Radiology* 2009;251:796-807.
17. Le Bihan D, Breton E, Lallemand D, Aubin ML, Vignaud J, Laval-Jeantet M. Separation of diffusion and perfusion in intravoxel incoherent motion MR imaging. *Radiology* 1988;168:497-505.
18. Le Bihan D, van Zijl P. From the diffusion coefficient to the diffusion tensor. *NMR Biomed* 2002;15:431-4.
19. Notohamiprodjo M, Glaser C, Herrmann KA, Dietrich O, Attenberger UI, Reiser MF, et al. Diffusion tensor imaging of the kidney with parallel imaging: Initial clinical experience. *Invest Radiol* 2008;43:677-85.
20. Ni H, Kavcic V, Zhu T, Ekholm S, Zhong J. Effects of number of diffusion gradient directions on derived diffusion tensor imaging indices in human brain. *AJNR Am J Neuroradiol* 2006;27:1776-81.
21. Cosottini M, Giannelli M, Vannozzi F, Pesaresi I, Piazza S, Belmonte G, et al. Evaluation of corticospinal tract impairment in the brain of patients with amyotrophic lateral sclerosis by using diffusion tensor imaging acquisition schemes with different numbers of diffusion-weighting directions. *J Comput Assist Tomogr* 2010;34:746-50.
22. Basser PJ. Inferring microstructural features and the physiological state of tissues from diffusion-weighted images. *NMR Biomed* 1995;8:333-44.
23. Rossi C, Boss A, Lindig TM, Martirosian P, Steidle G, Maetzler W, et al. Diffusion tensor imaging of the spinal cord at 1.5 and 3.0 Tesla. *Rofo* 2007;179:219-24.
24. Notohamiprodjo M, Dietrich O, Horger W, Horng A, Helck AD, Herrmann KA, et al. Diffusion tensor imaging (DTI) of the kidney at 3 tesla-feasibility, protocol evaluation and comparison to 1.5 Tesla. *Invest Radiol* 2010;45:245-54.
25. Kido A, Kataoka M, Yamamoto A, Nakamoto Y, Umeoka S, Koyama T, et al. Diffusion tensor MRI of the kidney at 3.0 and 1.5 Tesla. *Acta Radiol* 2010;51:1059-63.
26. Kataoka M, Kido A, Yamamoto A, Nakamoto Y, Koyama T, Isoda H, et al. Diffusion tensor imaging of kidneys with respiratory triggering: Optimization of parameters to demonstrate anisotropic structures on fraction anisotropy maps. *J Magn Reson Imaging* 2009;29:736-44.
27. Namimoto T, Yamashita Y, Mitsuzaki K, Nakayama Y, Tang Y, Takahashi M. Measurement of the apparent diffusion coefficient in diffuse renal disease by diffusion-weighted echo-planar MR imaging. *J Magn Reson Imaging* 1999;9:832-7.
28. Ries M, Jones RA, Basseau F, Moonen CT, Grenier N. Diffusion tensor MRI of the human kidney. *J Magn Reson Imaging* 2001;14:42-9.
29. Yoshikawa T, Kawamitsu H, Mitchell DG, Ohno Y, Ku Y, Seo Y, et al. ADC measurement of abdominal organs and lesions using parallel imaging technique. *AJR Am J Roentgenol* 2006;187:1521-30.
30. Le Bihan D, Breton E, Lallemand D, Grenier P, Cabanis E, Laval-Jeantet M. MR imaging of intravoxel incoherent motions: Application to diffusion and perfusion in neurologic disorders. *Radiology* 1986;161:401-7.
31. Le Bihan D. Theoretical principles of perfusion imaging. Application to magnetic resonance imaging. *Invest Radiol* 1992;27 Suppl 2:S6-11.
32. Lemke A, Laun FB, Simon D, Stieltjes B, Schad LR. An *in vivo* verification of the intravoxel incoherent motion effect in diffusion-weighted imaging of the abdomen. *Magn Reson Med* 2010;64:1580-5.
33. Zhang JL, Sigmund EE, Rusinek H, Chandarana H, Storey P, Chen Q, et al. Optimization of b-value sampling for diffusion-weighted imaging of the kidney. *Magn Reson Med* 2012;67:89-97.
34. Colagrande S, Belli G, Politi LS, Mannelli L, Pasquinelli F, Villari N. The influence of diffusion- and relaxation-related factors on signal intensity: An introductory guide to magnetic resonance diffusion-weighted imaging studies. *J Comput Assist Tomogr* 2008;32:463-74.
35. Muller MF, Prasad PV, Bimmler D, Kaiser A, Edelman RR. Functional imaging of the kidney by means of measurement of the apparent diffusion coefficient. *Radiology* 1994;193:711-5.
36. Damasio MB, Tagliafico A, Capaccio E, Cancelli C, Perrone N, Tomolillo C, et al. Diffusion-weighted MRI sequences (DW-MRI) of the kidney: Normal findings, influence of hydration state and repeatability of results. *Radiol Med* 2008;113:214-24.
37. Sigmund EE, Vivier PH, Sui D, Lamparello NA, Tantillo K, Mikheev A, et al. Intravoxel incoherent motion and diffusion-tensor imaging in renal tissue under hydration and furosemide flow challenges. *Radiology* 2012;263:758-69.
38. Reese TG, Heid O, Weisskoff RM, Wedeen VJ. Reduction of eddy-current-induced distortion in diffusion MRI using a twice-refocused spin echo. *Magn Reson Med* 2003;49:177-82.

Source of Support: Nil, **Conflict of Interest:** None declared.